NOISE CHARACTERIZATION UNCERTAINTY OF MICROWAVE DEVICES UNDER LOW CURRENT OPERATION

R. Lucero, C. Moyer, R. Vaitkus, and M. Dydyk

Motorola Phoenix Corporate Research Laboratories
Tempe, AZ 85283

ABSTRACT

An automated source reflection coefficient synthesizer combined with mechanical output tuner was used in conjunction with gage capability studies for the noise parameters of GaAs MESFETs and planar-doped psuedomorphic MODFETS operating at low currents (Ids <1 mA). The net repeatability and reproducibility (99 % confidence interval for the test) of the measurement system was established at ± 0.2 dB and ±1.4 dB for the minimum noise figure and associated gain, respectively.

INTRODUCTION

The objective of this work was to establish a methodology for the determination of noise parameters for field-effect devices operating at $I_{ds} \leq 1$ mA. Initial attempts to measure the noise parameters at 1 GHz of low-noise FETs repeatably by presenting known source impedances to the device, measuring the resulting noise figure and using a least squares technique to extrapolate the minimum noise figure (F_{min}) proved difficult for devices operating at low currents (I_{ds}=0.5 mA and V_{ds} =1.5 V). However, low current operation of microwave transistors has become increasingly important in portable radios and other applications requiring an extended battery life. Hence, accurate and repeatable noise parameter measurement methods are required for low current and noise MMIC design.

The system shown in Figure 1 employs an automated source reflection coefficient synthesizer capable of providing 16 different reflection coefficient states to the d.u.t. and a low loss mechanical output tuner to overcome the difficulty in the indirect measurement approach [1] - [4] of low gain devices exhibiting a high (≥ 0.9) output reflection coefficient.

Although the system used for this study operated at 1 GHz, the principle employed could be extended to higher frequency ranges. Typical values obtained for the noise parameters of 0.7 micron gate length GaAs MESFETs (NEC720) and in-house fabricated planar-doped pseudomorphic MODFETs under low current operation are given in Table 1. In this table, N_N is defined to be the normalized noise resistance and is given by [11]:

$$N_N = R_n G_{on} \qquad (1)$$

where R_n is the noise resistance and G_{on} is the real part of the optimum noise source admittance.

Gage capability [5] - [8] techniques were used in order to quantify the net repeatability (equipment variation) and reproducibility (inspector variation) of the test set and track system improvements. In this study, two inspectors performing 2 trials each made measurements on 10 randomly selected packaged units totalling 40 measurements per device class. The data obtained was used to derive an upper control limit for the process and determine the net repeatability and reproducibility (net r&r) figures of ±0.2 dB and ±1.4 dB for the minimum noise figure and associated gain, respectively. These limits establish a 99 % confidence interval (~5.19 standard deviations) for the test.

It is important to note that the use of an output tuner was not necessary to achieve a similar value for the net r&r for devices operating with an Ids ≥ 5 mA. Since these devices operating at higher currents exhibited an available gain ≥ 10 dB and a lower value for S_{22}, an investigation was made to determine the dependency of measurement uncertainty on the device's output mismatch and available gain under low current operation.

Noise figure measurement uncertainty can be attributed to second stage effects and d.u.t. available gain. The second stage effects are dominated by the d.u.t.'s output mismatch with the following dependency [4].

$$F_2\left[\Gamma_{OUT}\right] = F_2'\left[\frac{|1 - \Gamma_{OUT}\Gamma_{RCVR}|^2}{1 - |\Gamma_{OUT}|^2}\right] \qquad (2)$$

where Γ_{out} is the reflection coefficient looking to the left of reference plane 2 in Figure 1 and F_2' is the noise figure of the second stage measured with a well-matched noise source (i.e. $\Gamma_{out} \approx 0$). Γ_{RCVR} is the reflection coefficient measured to the right of reference plane 2. Thus, output mismatch loss must be included in the second stage noise figure of the measurement system. An increase in the second stage noise figure induces an error in the calculation of the d.u.t. measured noise figure when using Friss's equation [12]:

$$F_T = F_1 + \frac{F_2 - 1}{G_1} \qquad (3)$$

The graph shown in Figure 2 [9] is for the HP8970 noise figure meter and demonstrates the effect of the second stage noise figure on noise figure measurement uncertainty for a device with a 1.5 dB noise figure and with several gains. Note that for a measurement system noise figure of 5 dB, the measurement uncertainty can be as high as 0.4 dB for a device with an available gain of 10 dB. Hence, reduction of the system's second stage noise figure is very important when measuring low-gain devices.

SYSTEM DESCRIPTION

The system block diagram is shown in Figure 1. The impedance synthesizer utilizes coaxial microwave switches in conjunction with shorted stubs of varying

lengths and a termination to vary the impedance presented to the device. Source impedances reside in the upper half of the Smith chart. Due to excessive input tuner loss, a coupler is used in conjunction with a high ENR noise diode for noise injection into port 1 of the d.u.t. A low loss mechanical tuner at the output of the device is used to reduce the output mismatch and an extension of the network analyzer reference planes is made through a coupler and bias tee to accurately determine this tuner's output reflection coefficient as a function of source impedance state. This information is used for available gain error correction of the d.u.t.

The available power gain G_a, can be expressed as a function of the source admittance, Y_S, via:

$$\frac{1}{G_a[\,Y_s\,]} = \frac{1}{G_{max}} + N_g \frac{|\,Y_s - Y_{og}\,|}{G_s\,G_{on}} \qquad (4)$$

where $Y_S = G_S + jB_S$. Equation 4 can be expanded into a more convenient form for least-squares fitting G_a data taken for a number of different source admittances [13]:

$$\frac{1}{G_a[\,Y_s\,]} = A + B\frac{1}{G_s} + C\frac{B_s}{G_s} + D\frac{G_s^2 + B_s^2}{G_s} \qquad (5)$$

Where A, B, C, and D are the fitting constants. Once the constants are evaluated, equation 5 can be used to predict available gain under all conditions where G_S is not equal to zero; equation 4 is valid only for unconditionaly stable devices - devices with a finite G_{max}. Similarly, the minimum noise figure is extrapolated based on the 16 known source impedances via the familiar relationship:

$$F = F_{min} + \frac{R_n\,|\,Y_s - Y_{on}\,|^2}{G_s} \qquad (6)$$

The measurement system is completely automated and controlled by an HP9836 computer with in-house software. A menu driven interface is provided for the user for measurement and calibration. The system has the ability to drive several bias supplies, transfer data to a Macintosh environment, and support reference plane rotation for fixture de-embedding. D.u.t. oscillations are detected by measuring the noise figure twice at each source impedance state and checking for a difference ≥ 0.1 dB. In addition, drain current of the d.u.t. is monitored for fluctuations throughout the 16 source impedance cycle.

System calibration consists of measurements of source impedance states and associated input tuner losses, an output reflection meter calibration, and a second stage noise figure measurement. Initially, the network analyzer is calibrated at the APC-7 reference planes, the high ENR noise diode is turned off, and the tap port of the output coupler is terminated.

The 16 source impedances are then read with the network analyzer at plane 1 (Figure 1) and stored in memory. An HP346 noise source with a known ENR is then used to determine the noise contribution of the second stage (i.e. F_2' in Equation 1) by placing it at reference plane 2. The noise figure of this stage was typically 3 dB. The HP8970 noise figure meter was then used to determine the input tuner loss for each of the 16 source impedances by removing the transistor test fixture and the output tuner from the system and making an available gain measurement. Upon completion of the input tuner loss measurement, the HP8510 (0 dBm source power and 64 averages) was connected to the tap port of the output coupler and the calibration standards placed at plane 2. The calibration of the network analyzer was verified within the bandwidth of the coupler. The transistor test fixture and output tuner were then placed between reference planes 1 and 2. Although the output tuner was embedded in the device measurement it's loss was low and contributed little to the second stage noise figure ($F_2\,[\,\Gamma_{out}\,]$). Output tuner loss was measured with the HP8510 network analyzer to be between 0.2 and 0.7 dB for conjugate matching conditions as described by Strid [11]. A system improvement would be to replace the manual tuner with a computer controlled tuner of known loss capable of conjugately matching the d.u.t.'s output for each source impedance point.

In order to make a measurement, the device was placed in the fixture and bias applied, the output tuner was then used to conjugately match a typical device's output by monitoring the Smith chart display on the 8510 with the input tuner set to an impedance state near the expected Γ_{opt} for minimum noise. The tuner had to be tuned only once for each device class tested. Since $S_{12} \neq 0$ for the devices measured, variation in the source impedance produced a change in the output reflection coefficient which was monitored with the 8510. Source impedances producing: $\Gamma_{out} \geq .5$, $G_a \leq 5$ dB, or a measured noise figure in excess of 5 dB were removed from the curve fit routine. The state exclusion criteria for Γ_{out} was determined experimentally and by using Equation 2. For example, given $\Gamma_{out} = 0.9\,e^{j76°}$, $\Gamma_{RCVR} = .08\,e^{j-14°}$, and $NF_2' = 3$ dB ($F_2' = 1.99$), the effective second stage noise figure (NF_2) is 9.9 dB from Equation 2. This will cause an increase in the uncertainty of the noise figure measurement by about 1 dB for a device with 10 dB gain according to Figure 2. However, if $|\Gamma_{out}| = 0.5$ and the other variables are kept constant in Equation 1, the effective noise figure of the second stage is approximately 4 dB and does not impact measurement uncertainty to the same degree.

GAGE STUDY DESCRIPTION & METHODOLOGY

The gage capability study provided a systematic approach to quantify the noise figure measurement uncertainty of the test set. An example of the data sheet used in the study (obtained from General Motors) and the corresponding formulas used to derive the upper control limit and the net r&r are given in Figures 3 and 4 respectively. The constants used in the gage formulas were statistically derived and are dependent on the number of trials and the number of inspectors used in the study. Two inspectors were used in this study to derive a figure for the net r&r for each of the noise parameters.

Inspector A randomly measured 10 NEC720 devices and entered the results into column 1 of the check sheet. Inspector B repeated this step and the entire process cycled with the 10 parts measured in another random order. The average result for each trial by each inspector was determined and entered at the bottom of the column for the appropriate trial. This is shown as the level 1 average in Figure 3. The overall average result (level 2 average) for each inspector was then found. The range of measurements for each sample for each inspector was determined by taking the difference between the maximum and minimum reading for each sample. The average range for each inspector was computed and recorded at the bottom of the "Range" column.

The overall average range (.01905 in Figure 3) was determined by adding the range obtained for each inspector and dividing the result by the number of inspectors. The difference between the maximum and minimum level 2 average result obtained for the individual inspectors was determined and entered as AVE DIF (X_{DIFF}) in Figure 3. The upper control limit (UCL_r) for the range was computed by multiplying the average of the range, by the factor D_4. At this point individual ranges were inspected and those exceeding the UCL_r identified. The cause of the excessive variation was identified and corrected. The repeatability -- equipment variation -- and the reproducibility -- appraiser variation was then computed using the formulas in Figure 4.

EXPERIMENTAL RESULTS

The original system design did not include an output tuner and a gage capability check found the measurement process to be out of control (a statistically significant number of repeated measurements fell outside of a Gausian distribution) when evaluating devices under low current operation. However, when the operating current was increased to 5 mA, repeating the measurement process yielded data which followed a Gausian distribution.
Table 2 summarizes four different gage study results for 10 NEC720 devices under various test set configurations. Case A was for Ids = 5 mA, Vds = 2.5 V bias condition. Case A did not include an output tuner nor were any states excluded from the curve fit routine. Note that the 99 % confidence interval for this configuration was ±.2 dB and ±1.6 dB for noise figure and gain respectively. This became the benchmark figure for the test set. Case B was for a low bias condition (Ids = .5 mA, Vds = 1.5 V) and utilized the same test set configuration as Case A. Comparing the net r&r values for the two cases clearly shows the increase in the measurement uncertainty for the test. Case C shows the data for a low bias condition with the addition of the mechanical tuner at the d.u.t. output. The reduction in the noise figure measurement uncertainty is obvious however, there was a problem with associated gain net r&r. Case D utilized the same low current bias condition and the output tuner, but states producing an available gain ≤ 5 dB and $|G_{out}| \geq .5$, were omitted from the curve fit routine. The state exclusion criteria, and the addition of an output tuner, were responsible for reducing the uncertainty in the measurement to levels comparable to the high current bias condition.

CONCLUSION

Noise measurements of microwave transistors at low currents are dominated by second stage noise figure effects. A reduction in the output mismatch to values of $|\Gamma_{out}| \leq .5$, a requirement of gain>5 dB and a requirement of noise figure<5 dB for each source impedance state used in parameter extraction resulted in improved noise parameter repeatability as quantified by a reduction in the 99% confidence interval from ±0.6 dB to ±0.2 dB for noise figure.

ACKNOWLEDGEMENT

The authors wish to thank Dr. John Escher and Mr. Conrad Monroe for their encouragement and support of this work. We also wish to thank Theresa Hopson who was very helpful with the acquisition and analysis of the gage study data.

REFEERENCES

[1] R.Q. Lane, "The Determination of Device Noise Parameters,"*Proc. IEEE*, vol. 57, pp. 1461-1462, Aug. 1969

[2] M. Sannino, "On the Determination of Device Noise and Gain Parameters," *Proc. IEEE*, vol. 67, pp. 1364 - 1366, Sept. 1979

[3] V.A. Hirsch, M.D. Brunsman, and T.H. Miers, "An Automated System for De-Embedded Measurments of Noise and Gain Parameters" 29th ARFTG Digest, pp. 38 - 51, 1987

[4] Enrico F. Calandra, Giovanni Martines, and Mario Sannino,"Characterization of GaAs FET's in Terms of Noise, Gain, and Scattering Parameters Through a Noise Parameter Test Set" IEEE Transactions on Microwave Theory and Techniques, vol. MTT-32, No. 3, pp 231 - 236, March 1984

[5] Statistical Quality Control Handbook, Western Electric, Select Code 7000-444, PO Box 19901, Indianapolis, Ind 46219, (800) 432-6600

[6] Measurement System Analysis, Chevrolet Motor Division, GMC

[7] R. Travor, "Measuring Equipment Repeatability - The Rubber Ruler," 1962 ASQC Convention Transactions

[8] H.C. Charbonneau, "Industrial Quality Control," Prentice-Hall Inc., NY 1978

[9] Hewlett Packard Product Note 8970B/S-2, "Applications and Operation of the HP 8970B Noise Figure Meter and HP 8970S Microwave Noise Figure Measrement System," pp. 41

[10] E.W. Strid, "Measurement of Losses in Noise - Matching Networks," IEEE Transactions on Microwave Theory and Techniques, vol. MTT-29, pp 247 - 252, March 1981

[11] J. Lange, "Noise Characterization of Linear Two Ports inTerms of Invariant Parameters," IEEE Journal of Solid State Circuits, vol. SC-2, no. 2, pp. 37 - 40, June 1967.

[12] H.T. Friss, "Noise Figures of Radio Receivers," Proc. IRD, vol. 32, pp. 419 - 422, July 1944.

[13] M. Sanino, "Simultaneous Determination of Device Noise and Gain Parameters Through Noise Measurements Through Noise Measurements Only," Proc. IEEE, vol. 68, pp 1343 - 1345, October 1980.

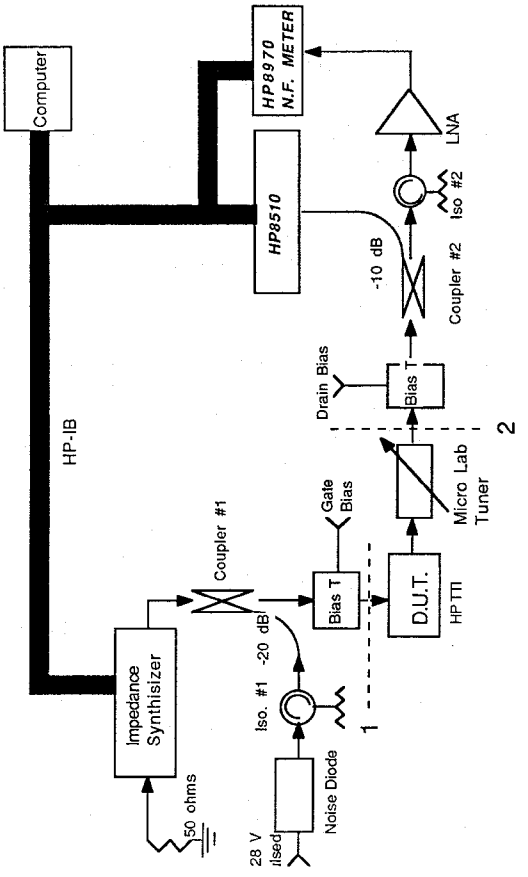

Figure 1 : Automated noise figure measurement system. Reference planes 1 and 2 correspond to the source reflection, and network analyzer, calibration planes respectively.

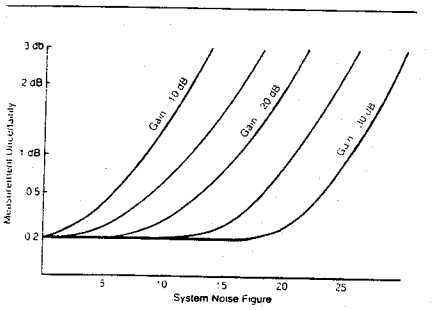

Figure 2: Measurement uncertainty vs. system noise figure for d.u.t. with a 1.5 dB noise figure and various gains [9].

Device	Freq. (Ghz)	Fmin (dB)	Nn	Gamma Opt (Lin)	Gamma Opt (Degrees)	Ga (@ Fmin) (dB)
NEC720	1	0.7	.09	0.95	23.2	7.6
MODFET	1	0.8	.12	0.80	13.5	11.4
NEC720*	1	0.9	.14	0.9	18.2	15.1

Table 1: Typical device noise parameters obtained with low current noise figure measurement system for Ids = 0.5 mA, and Vds = 1.5 V. NEC720* is for an Ids = 5 mA, Vds = 2.5 V bias condition.

Config.	Freq. (Ghz)	Fmin (dB)	Nn	Gamma Opt (Lin)	Gamma Opt (Degrees)	Ga (@ Fmin) (dB)
Case A	1	± .21	±.04	±.04	±2.6	±1.63
Case B	1	± .62	±.18	±.06	±.75	±3.1
Case C	1	±.32	±.05	±.03	±1.4	±3.0
Case D	1	±.21	±04	±.02	±1.3	±1.4

Table 2 : Net R&R summary for 1 GHz Noise Parameter Test Set.

Upper Control Limit (UCL_R)

$$UCL_R = R_{AVG}\left[D_4\right]$$

where $D_4 = 3.27$ or 2.58 for 2 or 3 trials, respectively, and R_{AVG} is given by:

$$R_{AVG} = \frac{R_{AVG\text{-}A} + R_{AVG\text{-}B}}{2}$$

Repeatability - Equipment Variation (E.V.)

$$E.V. = R_{AVG}\left[K_1\right]$$

where $K_1 = 4.56$ or 3.05 for 2 or 3 trials, respectively.

Reproducibility - Appraiser Variation (A.V.)

$$A.V. = \sqrt{\left[X_{DIFF} \times K_4\right]^2 - \left[\frac{E.V.^2}{n \times r}\right]}$$

where n is the number of parts, r is the number of trials, and $K_4 = 3.65$ or 2.70 for 2 or 3 inspectors, respectively.

Repeatability and Reproducibility (R&R)

$$R\,\&\,R = \sqrt{\left[E.V.\right]^2 + \left[A.V.\right]^2}$$

Figure 4 : Equations and constants used in the gage capability study.

Gage R and R data sheet for NOISE FIGURE (dB)
9/21/88 **LOW - CURRENT - CASE D**
MANTA 1 GHz noise figure measurement test set

INSPECTOR SEQUENCE:	A (1ST)		A (2ND)			B (3RD)		B (4TH)		
TRIAL	1		2			1		2		
ID#	ORDER TAKEN	Fmin (dB)	ORDER TAKEN	Fmin (dB)	RANGE	ORDER TAKEN	Fmin (dB)	ORDER TAKEN	Fmin (dB)	RANGE
NEC720_1	9	0.72	6	0.76	0.04	7	0.78	5	0.68	0.1
NEC720_2	5	0.82	4	0.85	0.03	5	0.83	1	0.81	0.02
NEC720_3	3	0.71	9	0.56	0.15	9	0.8	3	0.66	0.14
NEC720_4	7	0.69	3	0.63	0.06	3	0.73	7	0.63	0.1
NEC720_5	10	0.66	1	0.8	0.14	2	0.79	4	0.46	0.33
NEC720_6	2	0.8	7	0.82	0.02	8	0.85	10	0.67	0.18
NEC720_7	6	0.58	2	0.46	0.12	1	0.56	9	0.54	0.02
NEC720_8	1	0.73	5	0.68	0.05	10	0.8	6	0.8	0
NEC720_4	4	0.83	8	0.9	0.07	4	0.88	8	0.76	0.12
NEC720_5	8	0.77	10	0.64	0.13	6	0.8	2	0.8	0
Level 1 Avg. (L1A)		0.731		0.71	0.081 (RAVG - A)		0.782		0.681	0.101 (RAVG - B)
Level 2 Avg. (L2A=AVG(L1A))			A =	0.7205				B =	0.7315	

OPERATOR	L2A	R_AVG
A =	0.721	0.081
B =	0.732	0.101
AVE MIN	0.721	
AVE MAX	0.732	
AVE DIF	0.011	
AVE RANGE		0.091
UCLr		0.29757
REPEATABILITY		0.41496
REPRODUCABILITY		0
NET R&R		0.41496

Figure 3: Gage capability study data sheet for Case D.